

Homework 3: Simulations

Nicole Zattarin

Abstract

Simulations are fundamental in scientific research both to assert theoretical statements and to design an experimental setup, therefore multiple strategies have been explored in order to provide accurate results in a computationally feasible time. In this report we first explore the simulation of a single service queue system with Monte Carlo simulation and compute the corresponding metrics. In the second part we explore different scenarios of a system subjected to interference, exploiting both Monte Carlo simulation and numerical integration by means of Gaussian Quadrature Rules. Finally, we simulate a forwarding model and evaluate its performances.

1. SINGLE SERVICE QUEUE

Let us consider a single server queue, we perform a discrete-time simulation under the assumption that arrivals cannot leave in the same slot in which they arrive. We consider the following situations:

- (a) $P[1 \text{ arrival}] = P[2 \text{ arrivals}] = a$, $P[0 \text{ arrival}] = 1 - 2a$, $a \in [0, 0.5]$. and single service time for each user;
- (b) $P[1 \text{ arrival}] = P[0 \text{ arrival}] = 0.5$ and geometric service time with mean probability b .

We design a program that simulate a fixed number of time slots (10000 in our case) and computes the average throughput, delay, occupancy, arrival rate, service time and returns the whole history of the queue state. Moreover, we are interested in studying the stability of the queue, to do so we compute the utilization factor ρ , which is computed as follows:

$$\rho = \frac{\text{average arrival rate}}{\text{average service time}}. \quad (1)$$

From the previous definition it is pretty intuitive to understand that the condition for stability is the following:

- $\rho > 1$ the rate of arrivals cannot be compensated with the departure rate, i.e. service time is too long to serve enough users and the state diverges;
- $\rho = 1$ the rate of arrivals is equal to the service time, thus we would expect to observe the queue periodically getting empty for a while, but after a certain time it is likely that the status diverges.
- $\rho < 1$ the service time is such that it is possible to serve all users, thus the queue periodically empties because users arrived are quickly served.

Finally, to make our simulation more realistic, we implement a finite-size buffer system, such that if a new arrival would exceed the maximum queue size, it is dropped. This mechanism also allows to measure the overflow probability of a queueing system.

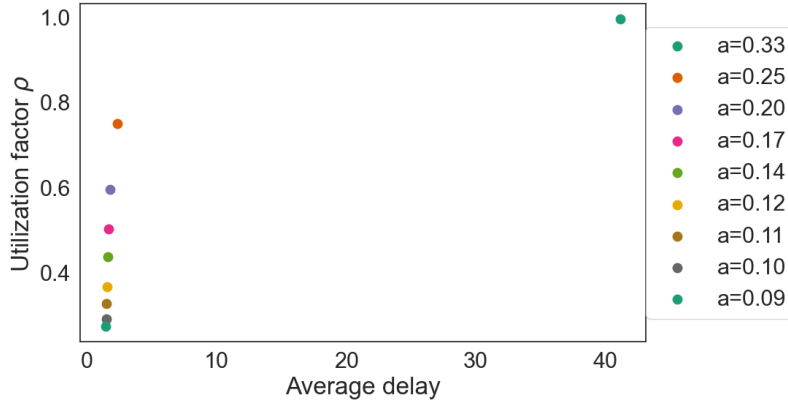


Figure 1: Queueing system with $P[1 \text{ arrival}] = P[2 \text{ arrivals}] = a$, $P[0 \text{ arrival}] = 1 - 2a$ and unitary service time, delay vs ρ by varying a from 0 to $1/3$.

1.1. Single service time - 0/1/2 arrivals

In case (a) the average service time is constant, thus the value of ρ depends on the arrivals rate: the more is the probability of observing 1 or 2 arrivals the larger will be ρ : $\rho \propto a$. Indeed, in Figure 1 we show delay, i.e. the time a user waits in the queue until it can be served, vs ρ by varying a from 0 to $1/3$. We can observe that ρ grows with the delay, while both delay and ρ increase with a . As we already pointed out, we would have expected to observe ρ increasing with a , since larger values of a correspond to a higher probability of observing 1 and 2 arrivals with respect to 0 arrivals. Moreover, delay increases with ρ since higher values of ρ , in the case of a fixed service time, correspond to an accumulation of users in the queue that are waiting to be served.

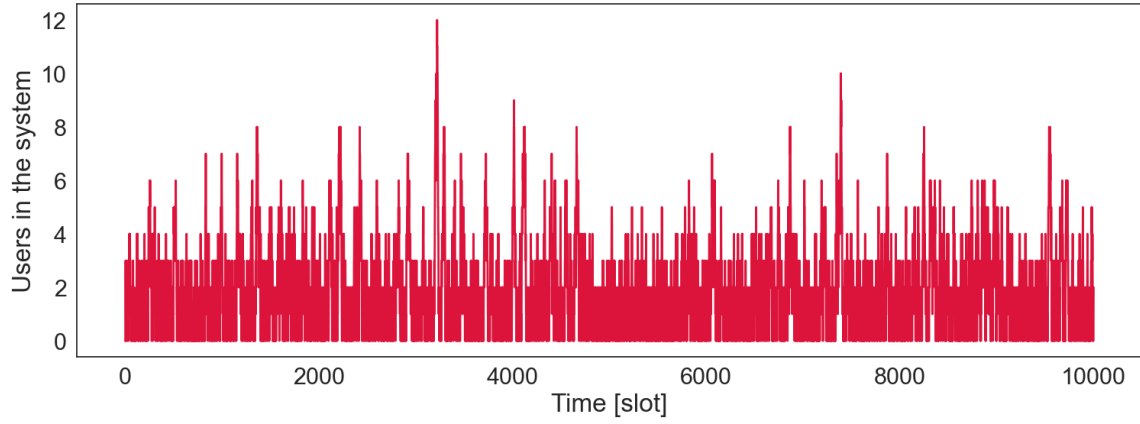
In Figure 2 we show the realization of queue size vs time for 10000 slots. Figure 2a shows results for $a = 1/4$, which corresponds to $\rho = 0.77$, thus to a stable queue. We can observe the expected behaviour for a stable system: the queue periodically empties, then new users are added and so on for a theoretically infinite time. On the other hand, figure 2b exhibits the same plot for $a = 1/3$, $\rho = 1$. In this case the behaviour is less stable, the queue status oscillates and the system empties once, but the general trend is increasing. Finally, Figure 2b shows the unstable simulation for $a = 1/2$, $\rho = 1.5$, in this case the probability of observing zero arrivals is null, while service time is still fixed to 1. As a consequence the number of users waiting to be served diverges.

1.2. Geometric service time - 0/1 arrivals

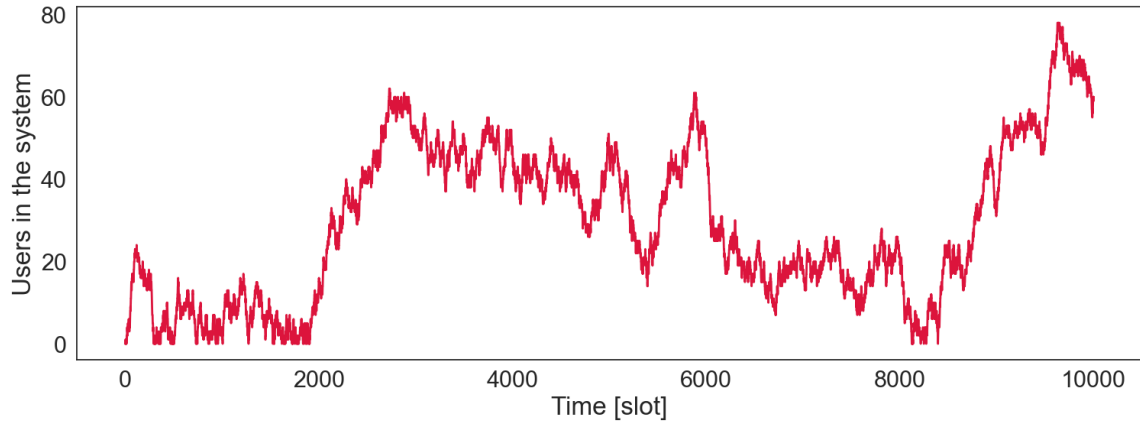
In case (b) the average service time is a geometric RV with mean value $1/b$, as a consequence the value of ρ depends on the parameter b . In this case we would expect the opposite behaviour: larger values of b correspond to larger faster service time in average and then to a faster processing of users in the queue.

In Figure 4 we show delay vs ρ by varying b from 0.5 to 1, as already introduced we observe that ρ grows with delay, while both delay and ρ decrease with b . Thus, in this case jobs are processed faster and users wait for less time in queue as b increases.

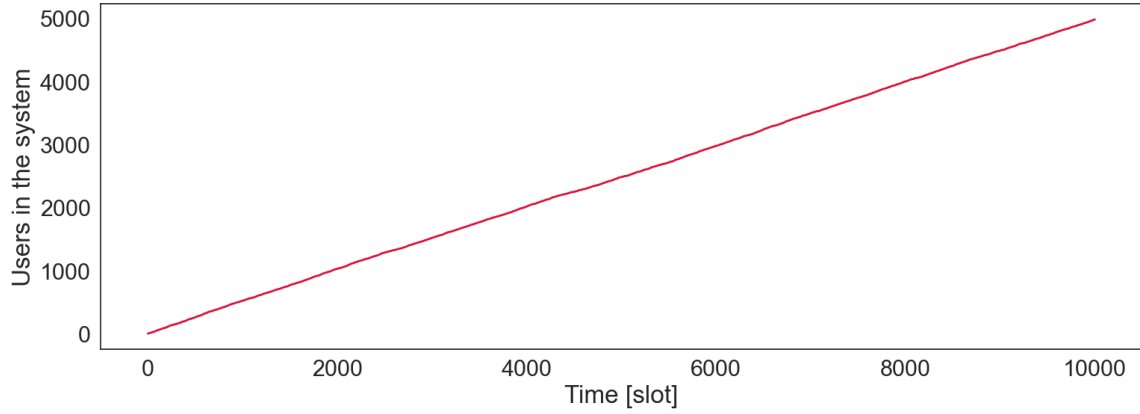
In Figure 4 we show the realization of queue size vs time for 10000 slots. Figure 4a shows results for $b = 1/3$ and $\rho = 1.50$, in Figure 4b we have $b = 1/2$ and $\rho = 1$, and in Figure 4c we have $b = 2/3$ and $\rho = 0.77$. In a completely analogous way as in case (a), but with the opposite trend, the previous cited figures denote respectively a non-stable, critical and stable queueing system.



(a) Queue size for a stable queueing system, $P[1 \text{ arrival}] = P[2 \text{ arrivals}] = 0.25$, $P[0 \text{ arrival}] = 0.5$, $\rho = 0.77$.



(b) Queue size for a critical queueing system, $P[1 \text{ arrival}] = P[2 \text{ arrivals}] = 0.33$, $P[0 \text{ arrival}] = 0.33$, $\rho = 1$.



(c) Queue size for an unstable queueing system, $P[1 \text{ arrival}] = P[2 \text{ arrivals}] = 0.50$, $P[0 \text{ arrival}] = 0$, $\rho = 1.5$.

Figure 2: Realization of queue size vs time for 10000 slots for different values of 1 and 2 arrivals probabilities, fixed service time.

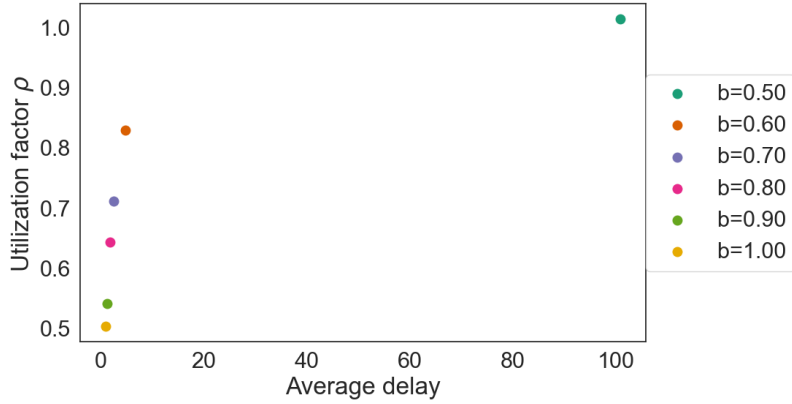


Figure 3: Queueing system with fixed 0 and 1 user arrivals probabilities and geometric service times with probability b , delay vs ρ by varying b from 0.5 to 1

| Case | Parameter | ρ | Buffer size for 0.001% overflow |
|------|-----------|--------|---------------------------------|
| (b) | $b=2/3$ | 0.77 | 8 |
| (b) | $b=1/2$ | 1 | 79 |
| (a) | $a=1/4$ | 0.77 | 8 |
| (a) | $a=1/3$ | 1 | 73 |

Table 1: Values of buffer sizes which guarantee a probability 0.001% of overflow for different stable simulations.

1.3. Overflow probability

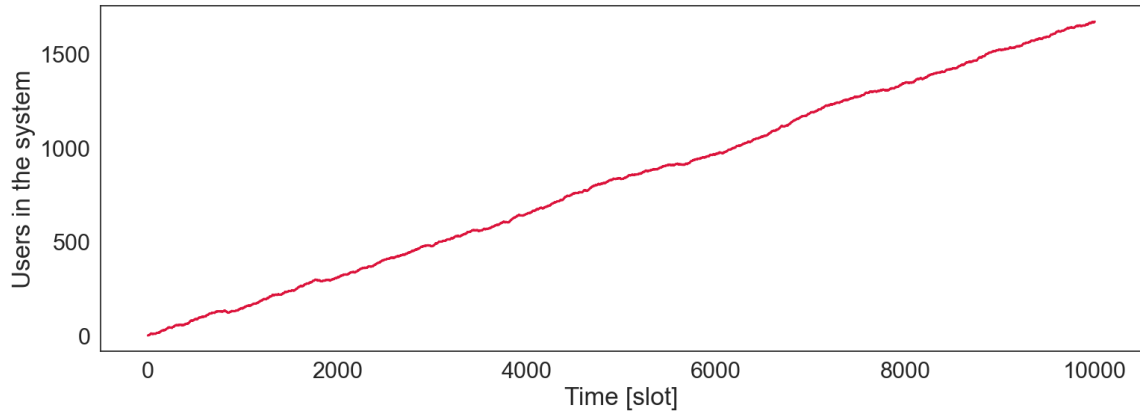
As we already pointed out, the service system is such that if the a new arrival would exceed the buffer size it is dropped. Before computing explicitly the buffer sizes necessary to guarantee a certain dropping probability, let us have a further look at Figures 4c and 2a. It is worth to highlight that the number of users in the system is constantly lower than 12 and, apart from a few isolated points, it is in general lower than 8.

We now want to be quantitative and perform a bisection root search to find the *integer* value of buffer size which guarantees a probability 0.001% of overflow, results for the cases $\rho \leq 1$ are reported in Table 1. The main outcome is that stable queues don't need a huge buffer capacity to provide a low dropping probability, while as the behaviour becomes more critical a larger queue is required. Finally, note also that results are similar, if not the same, for both simulations. This is not surprising, since the overflow probability depends on the nature of the system, if it is stable or not, so on the value of ρ , independently of the system employed to manage the queueing system.

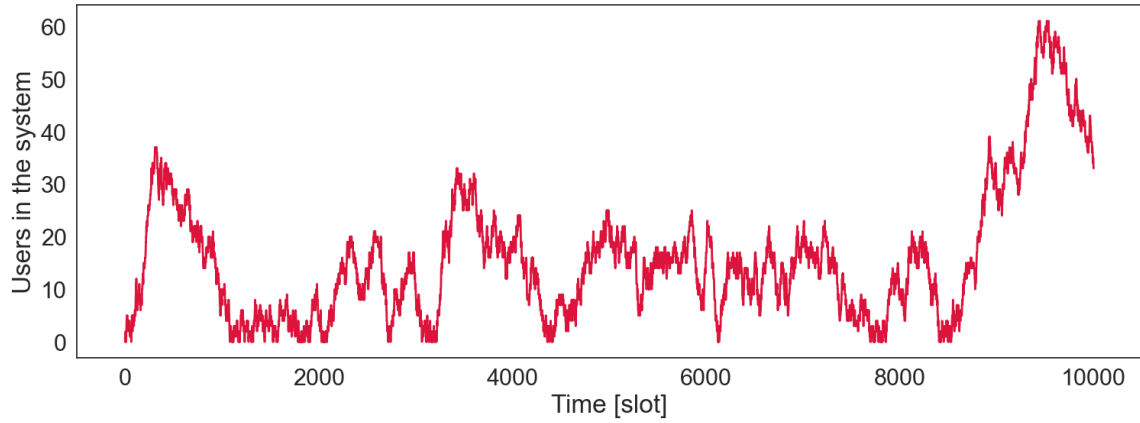
2. SINR PERFORMANCE

A useful quantity to measure the quality of a signal is the SINR (Signal to Interference and Noise Ratio), which basically takes into account the strength of the wanted signal compared to the unwanted interference and noise. Given a communication system affected by noise and interference, we want to evaluate its performances in terms of probability to correctly deliver the information, to do so, we compute the probability that the SNR is greater than a fixed threshold b :

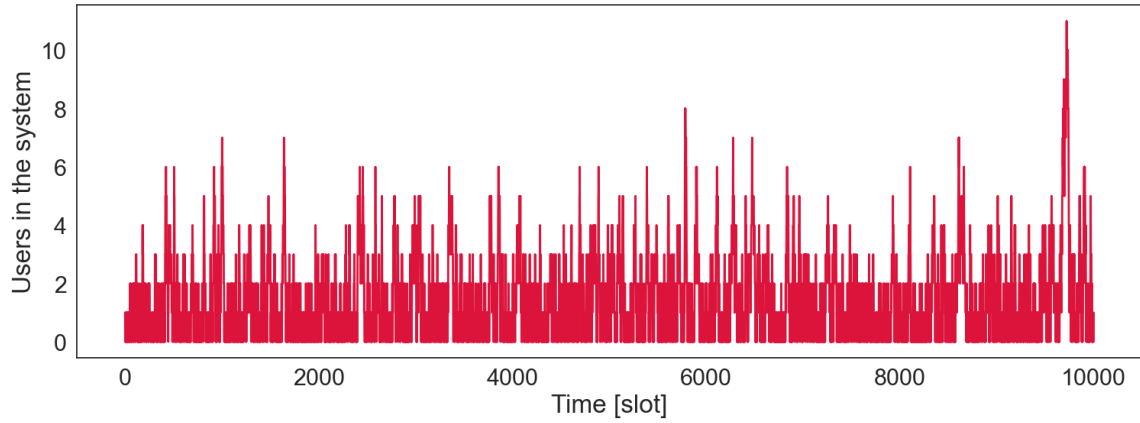
$$P_s = P[SNR > b], \quad (2)$$



(a) Queue size for an unstable queueing system, $P[1 \text{ arrival}] = P[0 \text{ arrivals}] = 0.5$, $b = 0.33$, $\rho = 1.5$.



(b) Queue size for a critical queueing system, $P[1 \text{ arrival}] = P[0 \text{ arrivals}] = 0.5$, $b = 0.5$, $\rho = 1$.



(c) Queue size for a stable queueing system, $P[1 \text{ arrival}] = P[0 \text{ arrivals}] = 0.5$, $b = 0.67$, $\rho = 0.77$.

Figure 4: Realization of queue size vs time for 10000 slots for fixed values of 1 and 0 arrivals probabilities, geometric service times with different probabilities.

where we refer to b also as capture ratio. Moreover, P_s can be computed analytically as follows:

$$P_s(r_0) = \int_{-\infty}^{+\infty} \frac{d\xi_0}{\sqrt{2\pi}\sigma} e^{-\frac{\xi_0^2}{2\sigma^2}} [I(\xi_0, r_0)]^k, \quad (3)$$

$$I(\xi_0, r_0) = \int_{-\infty}^{+\infty} \frac{d\xi}{\sqrt{2\pi}\sigma} e^{-\frac{\xi^2}{2\sigma^2}} \int_0^1 \frac{h(r)dr}{1 + be^{\xi - \xi_0(\frac{r}{r_0}) - \eta}},$$

where r_0 is the position of the intended user, r is the distance of the k interferers. Moreover, ξ_0 and ξ are normally distributed with zero mean and σ^2 variance. To solve the problem, i.e. to find Equation 2, two possible approaches are computationally feasible:

- Montecarlo simulation: randomly generate multiple times the involved variables with the required statistic and compute the frequency of the event $SNR > b$;
- Gauss Quadrature Rules to compute the integral in Equation 3.

The system described is still generic and can be used to approach different physical systems, we will focus on the following scenarios:

- Packet radio: a packet has to be delivered to an intended user, which is in an area characterized by a poisson distribution of interferers, r_0 is fixed, while r is in $[0, \infty)$;
- Cellular systems: an hexagonal cell is surrounded by cells of the same kind, located every 60° , in this case we are interested in computing the outage probability, r_0 is assumed uniform in the cell, while r follows the distribution of interferers;
- ALOHA: a multi access system in similar to the packet radio scenario, but in which every user can be potentially the intended or an interfere. We compute the throughput, considering a total area of radius $R = 1$.

We will describe more precisely these situation in the following sections.

2.1. Packet radio

Let us consider an intended user located at r_0 from the source and k interferers with $k \sim \text{Poisson}(\lambda\pi R^2)$, in a circular area of radius R . Interferers are located at distance $r = R u^{1/2}$ with $u \sim \mathcal{U}(0, 1)$ and all the other variable are distributed as already discussed.

In this scenario, equation (3) takes the form:

$$P_s(r_0) = \int_{-\infty}^{+\infty} \frac{d\xi_0}{\sqrt{2\pi}\sigma} e^{-\frac{\xi_0^2}{2\sigma^2}} e^{-\lambda\pi R^2\theta(\xi_0, r_0)} \quad (4)$$

$$\theta(\xi_0, r_0) = 1 - I(\xi_0, r_0) = \int_{-\infty}^{+\infty} \frac{d\xi}{\sqrt{2\pi}\sigma} e^{-\frac{\xi^2}{2\sigma^2}} \int_0^R \frac{\frac{2r}{R^2} dr}{1 + be^{\xi - \xi_0(\frac{r}{r_0}) - \eta}},$$

where λ is the density of interferers in a given circular area. We perform the numerical integration of (4) and the MC simulation with $r_0 = 10$ and $R = 100$, $\eta = 4$, $\sigma = 8\text{dB}$, both $b_1 = 6\text{dB}$ and $b_2 = 10\text{dB}$. Note, for this case and all the following sections, that all the theoretical results are in base e , while parameters are given in dB, thus we need to multiply them for a factor $\gamma = 0.1 \ln(10)$.

In Figure 5 we plot in log scale the success probability vs the density λ for all the discussed cases, Monte Carlo simulation in Figure 5a and numerical integration in 5b. We can highlight that a higher threshold corresponds to lower probability, as expected, and that the success probability decreases with the density of interferers. Both these results are intuitive, since as the number of interferers increase the probability that a package doesn't arrive to destination obviously decreases.

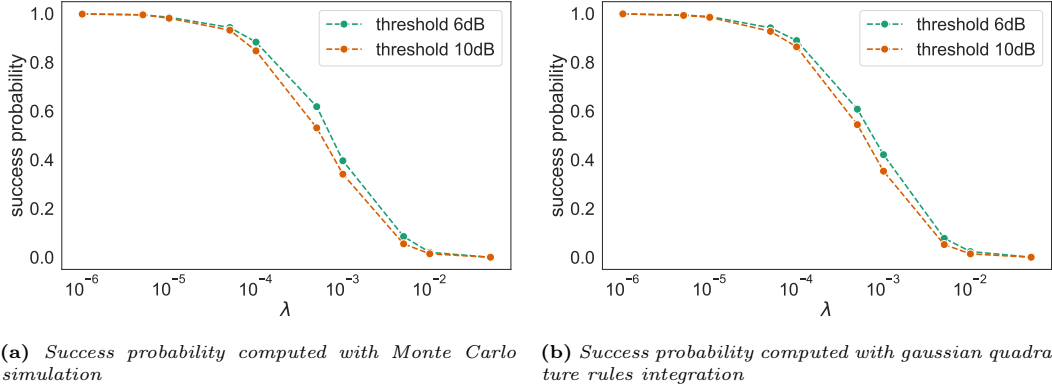


Figure 5: Packet radio scenario, success probability vs density λ of interferers in log scale for both the numerical integration and the Montecarlo simulation.

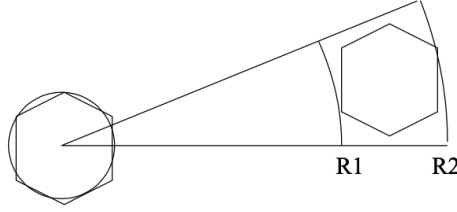


Figure 6: Schematic representation of the approximation introduced to compute numerically the integral for the cellular system

2.2. Cellular system

Let us consider a cell, in which we aim to deliver a message at location r_0 inside the cell, and k interferer cells with $k \sim B(n, \alpha)$, cells repeat each other every 60 degrees. In order to perform the simulation, instead of integrating (or generating RVs) over an hexagon, we consider a central circular cell of radius R and an interferer cell whose lower angle is at distance R_1 and the upper one is at distance R_2 , a schematic representation is provided in Figure 6.

In this scenario, equation (3) takes the form:

$$P_s = \int_{-\infty}^{+\infty} \frac{d\xi_0}{\sqrt{2\pi}\sigma} e^{-\frac{\xi_0^2}{2\sigma^2}} \int_0^R dr_0 \frac{2r_0}{R^2} (1 - \alpha \theta(\xi_0, r_0))^6 \quad (5)$$

$$\theta(\xi_0, r_0) = 1 - I(\xi_0, r_0) = \int_{-\infty}^{+\infty} \frac{d\xi}{\sqrt{2\pi}\sigma} e^{-\frac{\xi^2}{2\sigma^2}} \int_{R_1}^{R_2} \frac{\frac{2r}{R_2^2 - R_1^2} dr}{1 + b e^{\xi - \xi_0} \left(\frac{r}{r_0}\right)^{-\eta}},$$

where α is the probability an interfering channel is used.

We perform the numerical integration of (5) and the MC simulation averaging over r_0 with $R = 0.91$, $\eta = 4$, $\sigma = 8\text{dB}$, both $b_1 = 6\text{dB}$ and $b_2 = 10\text{dB}$. In Figure 7 we show the outage probability vs the parameter α . As in the previous case, a higher threshold corresponds to higher outage probability, and outage probability grows with the parameter considered.

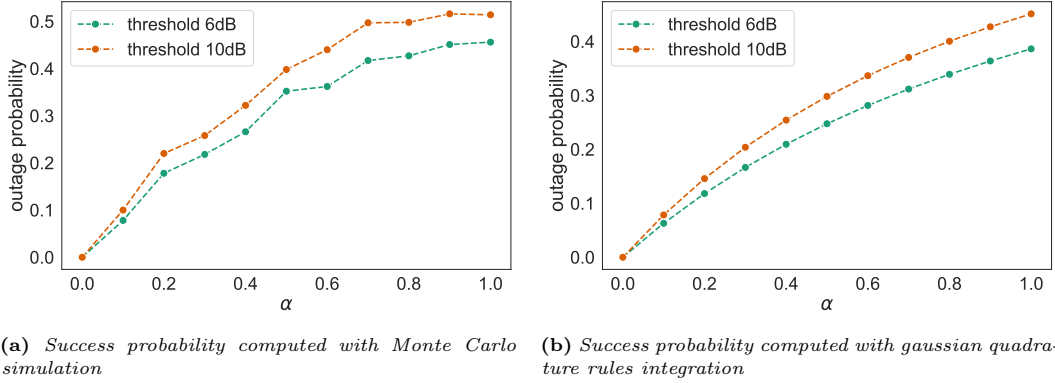


Figure 7: Cellular scenario, outage probability vs parameter α , i.e. probability that a channel is interfering, for both the numerical integration and the Montecarlo simulation.

2.3. ALOHA

Let us consider a the packet radio scenario, but in this case each user can potentially be either the intended one or an interferer, thus the probability of success in a slot is at most 1, and the event associated with the success of different users are independent. The average number of successes per slot S , which physically represents the throughput, can be computed from the usual integration as follows:

$$S = \int_{-\infty}^{+\infty} \frac{d\xi_0}{\sqrt{2\pi}\sigma} e^{-\frac{\xi_0^2}{2\sigma^2}} \int_0^1 dr_0 \frac{2r_0}{R^2} G e^{-G\theta(\xi_0, r_0)} \quad (6)$$

$$\theta(\xi_0, r_0) = 1 - I(\xi_0, r_0) = \int_{-\infty}^{+\infty} \frac{d\xi}{\sqrt{2\pi}\sigma} e^{-\frac{\xi^2}{2\sigma^2}} \int_0^R \frac{\frac{2r}{R^2} dr}{1 + b e^{\xi - \xi_0} \left(\frac{r}{r_0}\right)^{-\eta}},$$

where G is the average number of transmission per slot.

To observe the behaviour of such system we integrate Equation (5) and perform MC simulation averaging over r_0 with $R = 0.1$, $\eta = 4$, $\sigma = 8\text{dB}$, both $b_1 = 6\text{dB}$ and $b_2 = 10\text{dB}$. In Figure 8 we show the throughput vs G , the main outcome is that, as we would expect, throughput decreases as the number of transmissions per slot grows and that higher thresholds correspond to lower throughput.

Finally, for a GQR integration, we plot the capture probability vs the collision size n , results are shown in Figure 9.

3. GERAF MULTIHOP PERFORMANCE

In this section we reproduce the results proposed in [1] and compare the Geographic Random Forwarding (GeRaF) model performances with GAF [2], see also [3] for further analysis. In particular, we implement GeRaF algorithm for the estimation of the average number of hops needed per the forwarding. In Figure 10 we exhibit the average number of hops with the respective standard deviations vs average number of active nodes for different distances, averages are computed over a sample of 100 simulations results. In particular, we can observe that GeRaF performs better than GAF best case for a reasonable number of active nodes. Moreover, the number of hops quickly decreases up to about 10 nodes and then almost get stabilized on a value which depends on the distance, but that is still better than GAF in any case.

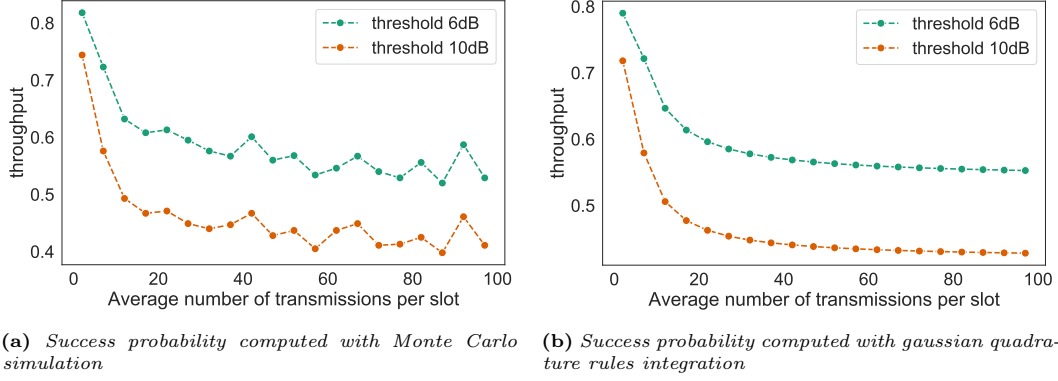


Figure 8: Multi access scenario, throughput vs average number of transmissions per slot G for both the numerical integration and the Montecarlo simulation.

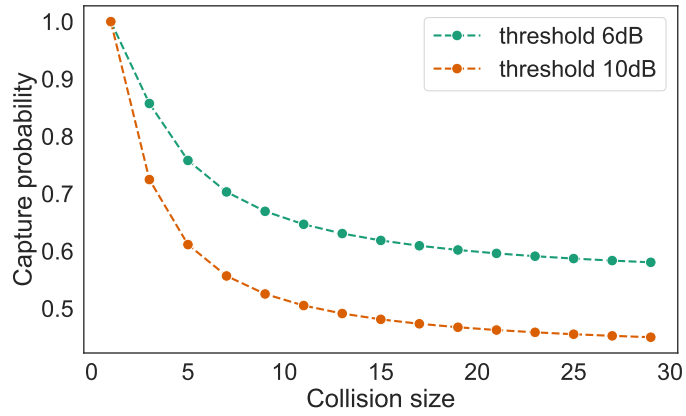
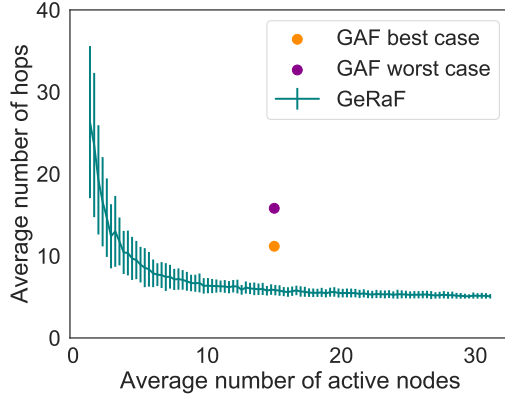
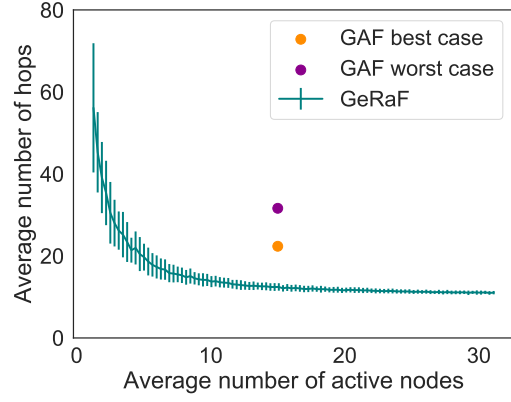


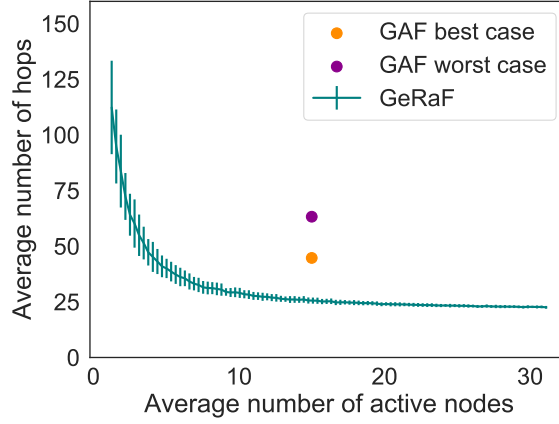
Figure 9: Capture probabilities as a function of N for different values



(a) Average number of hops vs average number of active nodes for $D = 5$.



(b) Average number of hops vs average number of active nodes for $D = 10$.



(c) Average number of hops vs average number of active nodes for $D = 20$.

Figure 10: Average number of hops and respective standard deviation vs average number of active nodes for different distances between sources and destination.

REFERENCES

- [1] ZORZI M. Geographic random forwarding (geraf) for adhoc and sensor networks : Multihop performance. *IEEE Trans. Mobile Comput.*, 2(4):337–365, 2003. URL <https://cir.nii.ac.jp/crid/1571980075820873728>.
- [2] Ya Xu, John Heidemann, and Deborah Estrin. Geography-informed energy conservation for ad hoc routing. In *Proceedings of the 7th Annual International Conference on Mobile Computing and Networking*, MobiCom '01, page 70–84, New York, NY, USA, 2001. Association for Computing Machinery. ISBN 1581134223. doi: 10.1145/381677.381685. URL <https://doi.org/10.1145/381677.381685>.
- [3] M. Zorzi and R.R. Rao. Geographic random forwarding (geraf) for ad hoc and sensor networks: energy and latency performance. *IEEE Transactions on Mobile Computing*, 2(4):349–365, 2003. doi: 10.1109/TMC.2003.1255650.